# Simultaneous $CO_2$ capture and metal purification from waste streams

Jean Septavaux,[1] Clara Tosi,[1] Patrick Jame,[2] Carlo Nervi,[3] Roberto Gobetto[3] & Julien Leclaire[1]*

**The process of carbon capture, which is one of the most mature yet cost-intensive technology proposed to mitigate global warming has herein been explored as a potential strategy to generate dynamic ligands for metals separation and recovery. Spontaneous $CO_2$ fixation by industrial polyamines such as diethylenetriamine affords dynamic arrays of interconverting species, from which tailored subsets can be selected yielding organometallic adducts of contrasted solubility. Quantitative compositional analyses of the phases produced with varying $CO_2$ loadings allowed to propose the underpinning self-sorting scenario induced by each metal, and to identify the conditions affording optimal individual separation by precipitation. To illustrate the potentiality of this approach, which could bring substantial added value into $CO_2$ capture and utilization chain value, bimetallic separation was conducted directly from the exhaust gas of an internal combustion engine vehicle, and the three constituents of the alloys used to produce the cathodes of electric vehicles were separated and recovered by successive $CO_2$-induced selective precipitations. This study provides a potential framework to integrated $CO_2$ capture and utilization and paves the ways toward the design of $CO_2$-sourced sustainable processes.**

During the last decade, the reduction of $CO_2$ emissions into the atmosphere has become one of the major challenges faced by humanity. The current objective is to maintain the global warming below a +2°C level with respect to the pre-industrial era, to avoid reaching a climate point of no return[1]. If the long-term solution undoubtedly relies on renewable energies, during the transition period which may last several decades, carbon capture and storage or utilization (CCS or CCU) will play a key role to stay on course.[2] Once captured, $CO_2$ has to be stored, ideally for the longest possible period and as high value-added products meeting a strong demand. In addition to chemically sequester carbon dioxide away from the atmosphere, utilization is indeed expected to economically counter-balance the cost of capture. Hence is CCUS undoubtedly a multifaceted issue, which requires a multidisciplinary approach to integrate the socio-economic and environmental dimensions to the scientific and technological challenges.

So far, industrial facilities deployed on large scale for $CO_2$ capture were mostly based on post-combustion scrubbing using aqueous amine absorbents. While this technology benefits from almost a century of scientific maturity,[3,4] its main viable economic model to date implies the use of the $CO_2$ purified and compressed for subsequent enhanced oil recovery (EOR). Despite being remarkably efficient from a thermodynamic point of view, this capture process requires such capital investments and operational expenditures (> 2.4 GJ/tonne), that no other alternative CCU chain of value could be proposed to date.[5,6] Recent studies on the latest generations of solvents and advanced process configurations[7] reveal that the margin for OPEX reduction is low, due to the dispersion of energy losses between many unitary operations devoted to fluids management. Consequently, any game-changing strategy should either entirely revisit the architecture of the capture process and/or couple it with high added value and low imprinting utilizations.

With this aim, we herein propose to valorize the adducts directly obtained from $CO_2$ capture for enhanced commodity production as a way to encourage industry to adopt CCUS. We indeed demonstrate that $CO_2$-rich solutions generated from

[1] Univ Lyon, Université Claude Bernard Lyon 1, CNRS, CPE Lyon, INSA, ICBMS UMR 5246, F-69611, Lyon, France.
[2] Univ Lyon, Université Claude Bernard Lyon 1, CNRS, ENS Lyon, ISA UMR 5280, F-69611, Lyon, France.
[3] Univ Turin, Dept Chemistry, 10125, Turin, Italy.

industrial amines are original molecular systems of metal ligands. Composition and ligating properties of these solutions can be tuned by physical stimuli in mild conditions, paving the way toward the design new sustainable processes for metal recovery. In the global chain, utilization of captured $CO_2$ for metal recovery may be one of the judges of peace, allowing to inject some substantial added value between capture and transformation, thereby leading to the development of new integrated capture and utilization processes.

$CO_2$ is a quadrupolar C-electrophile which reversibly reacts with a large panel of nucleophiles upon their deprotonation by a Bronsted base, generally delivering [oxyanion – protonated base] ion pairs. In water, primary and secondary amines gradually yield ammonium carbamates, then carbonates with increasing $CO_2$ loading and convert back into the initial reactants upon temperature increase and/or pressure drop. Ammonium carbamates, the products of $CO_2$ capture, have been considered as starting material[8,9] and intermediates for the production of $CO_2$-sourced commodities and by us and others as metal ligands[10] for the design of hydrometallurgic processes,[11] or the formation of hybrid materials.[12] The capture process itself can be valorized as a switch between two states of contrasted chemical and physical properties,[13] and be integrated into innovative technologies.[14,15]

We hypothesized that two classes of waste-containing effluents, namely the solutions obtained from $CO_2$ capture and metal leachates originating from end-of-life technological products could serve to build double level dynamic combinatorial libraries (based on carbamate and metal ligand exchange, scheme 1).[16] Such complex molecular networks were intended to provide, for each metal, a different combination of ligands and counter-ions yielding thermodynamically optimized yet compositionally different complexes. Selective binding to a highly charged species such as a $CO_2$-amine adduct is likely to yield a coordination complex with radically different physical properties than the naked metal cation, thereby allowing its straightforward separation from the starting mixture. To reach these objectives, a sufficient degree of ligand diversity must be generated through the spontaneous and reversible connection between $CO_2$ and the capture agent. This was achieved using diethyenetriamine (DETA), an industrial polyamine, for which non-, mono- and dicarbamated species were reported to co-exist upon capture from flue gas models, forming complex mixtures.[17]

**Polyamine-CO₂ as metal responsive systems**
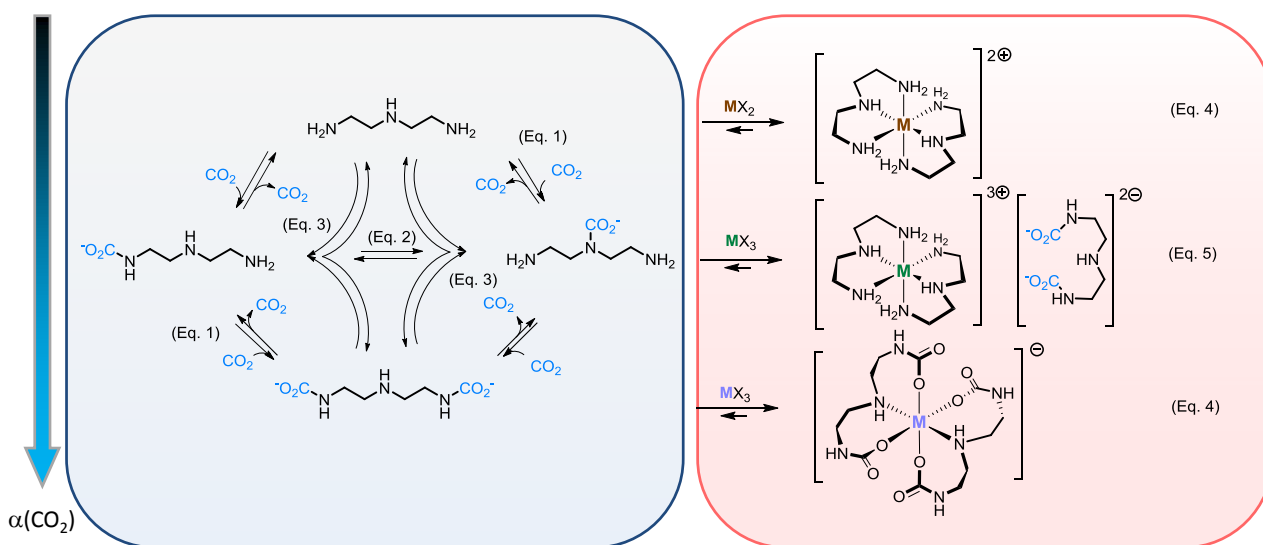


**Scheme 1. CO₂-loaded solution as dynamic constitutional libraries of ligands**. Reversible carbamate bond formation/cleavage (Eq. 1), exchange (intramolecular: eq. 2 and intermolecular, disproportionation: eq. 3) and fictitious metal-ligand binding in the first and second coordination spheres (Eq. 4 –5). Proton and inorganic counter-ions exchange processes were omitted for clarity.

With polyamines, two categories of equilibria involving the carbamate C-N bond and regulating the composition of solutions resulting from capture can be potentially affected by the introduction of an additional species such as a metal salt:

- C-N formation / cleavage (carbamation; scheme 1, Eq. 1) can be further favored, affecting the global loading if the gas is continuously supplied. We and others have indeed previously shown that organic or inorganic species reversibly binding amines or carbamates, can respectively act as carbamation antagonist or agonist, favoring either capture from dilute emissions[18,19] or stripping at low enthalpic costs.[20,21]

-C-N bond exchange can in principle occur at fixed $CO_2$ loading through *intra-* and/or *inter*molecular substitution reactions (transcarbamation; scheme 1, Eq. 2 and Eq. 3). Unlike the previous case, this exchange process is almost isoenergetic, hence preferable to observe the amplification of an assembled ligand upon selection and binding by a metal (Scheme 1, Eq. 4 and 5). Although no amplification was evidenced, we recently showed that oxophilic metal cations could, upon counter-anion exchange, selectively bind and co-precipitate the dicarbamates from such a library, while aminophilic metals mostly remained in solution.[22]

Metal-induced amplification was herein quantified by monitoring and comparing the $CO_2$-induced speciation of DETA by ^{1}H and ^{13}C NMR spectroscopy (qNMR) in the presence and absence of various pre-solubilized metal chlorides as leachate models. The first analyses were performed in methanol, a relevant solvent to observe the selective precipitation of metallo-carbamate adducts for subsequent extractive purification. In agreement with earlier reports,[23] the asymmetric monocarbamate **1a** is the dominant species at low loading in the absence of inorganic binder. More surprisingly is the tightly concomitant increase of the symmetrical mono- and dicarbamate species **1s** and **2s** with $CO_2$ loading (fig. 1a).

The virtual dynamic combinatorial library[24] which can be generated from DETA and $CO_2$ gathers around 20 objects differing from their protonation and carbamation state, providing contrasted binding ability (scheme 1).[17] Previous thermodynamic modelling considering the members of this array as independent species failed to simulate the experimental populations observed in water. In methanol, the system could be satisfyingly ($R^2 = 0.996$) depicted by a population of four dominant species related by three equilibria ($K_{1a} = 48$ L.mol$^{-1}$; $K_{1s} = 6.1$ L.mol$^{-1}$; $K_6 = 277$ L$^2$.mol$^{-2}$). This simplistic thermodynamic model which reasonably fits the experimental data allowed to draw a preliminary molecular scenario of the progressive capture of $CO_2$ by DETA. First, unprotonated DETA mainly converts into asymmetric zwitterionic monocarbamate **1a** (fig. 1c, Eq. 1a) and, to a lesser extent, **1s** (fig. 1c, Eq. 1s). Upon further loading, the former binds a second molecule of $CO_2$ and converts into **2s**$^-$ upon deprotonation by **1s**,[25] leading to a tricarbamate double strand **1s**$^+$:**2s**$^-$ (Eq. 6).[26] This final favorable pairing, which could be observed experimentally by cryo-ESI-MS and ^{1}H DOSY NMR and *in silico* by DFT calculations at the B3LYP-D3BJ/def2TZVP level (fig. 1b and supplementary material fig. S1), displaces the two preceding unfavorable steps.
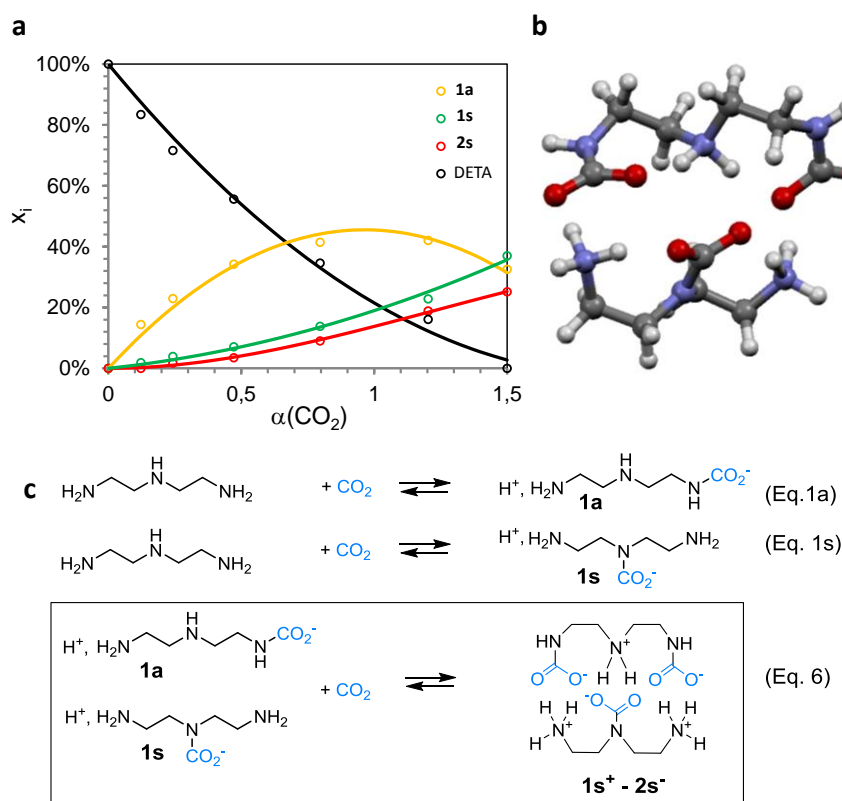
**Figure 1. Untemplated dynamic combinatorial system based on DETA and $CO_2$.** a. $CO_2$-induced speciation of DETA in $CD_3OD$. DETA (black), asymmetrical mono **1a** (yellow), symmetrical mono- (green) **1s** and dicarbamate **2s** (red). Dots: experimental points, line: simulated values from the thermodynamic model based on equilibria (1) – (3) fitted values of equilibrium constants and (b) DFT modelling of (**1s⁺:2s⁻**) at the B3LYP-D3BJ/def2TZVP level.

In the absence of metal, this non-covalent pairing process is the main thermodynamic driving force which regulates the population of the system. The organic double strand is indeed the major species at high loading (50 % of the library at $\alpha$ = 1.5). With the $N^4$-methylated mutant of DETA, which cannot form the symmetrical template strand **1s** (Supplementary material fig. S2), the $CO_2$-induced speciation reveals an identical trajectory for **1a**, while **2s** is substantially less favored and replaced by carbonated DETA. This latter species indeed dominates the population at high loading. **1s⁺:2s⁻** pairing therefore seems to preserve the DETA-based system from carbonation due to moisture at high loading. Although being designed to be isoenergetic and thereby easily perturbed by metal coordination, the carbamate exchange is biased by an unexpected highly stabilizing pairing process. This phenomenon may act as a thermodynamic counter-driving force opposing to the preferential complexation of a member of the DETA-$CO_2$ system with a metal partner.

Rare earth (RE) metals were first investigated for their ability to perturb the composition of the DETA-$CO_2$ system by preferential binding to one of its members. Yttrium was selected as representative of the series providing the optimal resolution for *in situ* qNMR, while *ex situ* analyses were conducted with lanthanum and yttrium (*vide supra*). In agreement with our previous report,[20] the rare earth elements proved to induce identical partitioning effects on the various building blocks used. In the presence of 1/12 eq. $RECl_3$, the maximal amount of template affording a fully reversible system,[20,27] *i.e.* on which $CO_2$ can still be expelled by thermal stripping, precipitation starts around $\alpha_S(CO_2)$ = 0.20. The molecular composition of the resulting solid, which appeared to be amorphous from powder X-ray and solid-state NMR analyses, was determined *ex situ*, *i.e* after isolation by quantitative hydrolysis of the reversible linkages and titration of each class of building block released by a separate analytical technique ($CO_2$: volumetry; DETA: $^1H$ quantitative NMR (qNMR); metal: ICP-OES; chlorine: ionic chromatography).[21] In terms of partition (figure 2a), the fractions of amine, metal and chlorine incorporated

into the solid rapidly rise to maximal values of respectively 15 %, 95% and 3% of the initial amounts introduced. Concomitantly, the $CO_2$ loading of the solid phase continuously increases from 1.5 to 1.95. These asymptotic values can be translated into a raw molecular formula $RE(DETA)_2(CO_2)_4$ which may be re-written as $RE(\mathbf{2s})_2H$.
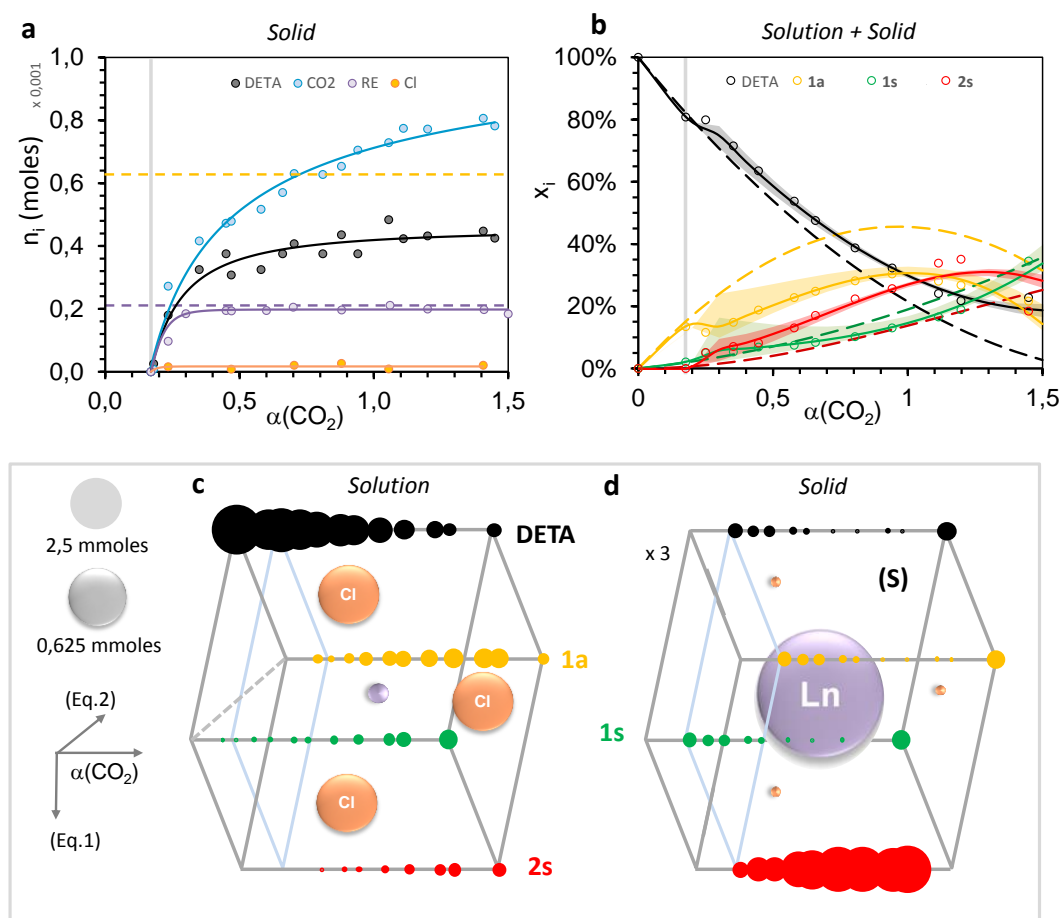


**Figure 2. Constituent analyses of the $RECl_3$-DETA-$CO_2$ ternary system in MeOH.** (a) $CO_2$- induced capture of the various building blocks (in mmol) with increased loading from 2.5 mmol of a DETA: $RECl_3$ 1:0.083 system. Dotted lines represent the amounts initially introduced and vertical solid lines materialize the precipitation process. (b) Proportions of the four major organic species in the solid + liquid system plotted with $CO_2$: DETA loading: (dots: experimental points, line: polynomial fitting; beams: maximal statistical dispersion in the solid; dotted line: reference system in the absence of $RECl_3$). 3D combined representation of the organic DETA-$CO_2$ species on the vertices with increasing $CO_2$ loading from left to right in the liquid phase (c) and in the solids (d, scaled up x3). Surfaces of the disks quantify the amount of each species (metal and chloride values correspond to the asymptotes displayed in part (a).

For any loading, the global population in $CO_2$-amine adducts can be reconstituted from the data collected for each phase. *In situ* qNMR analyses of the supernatant allow to precisely quantify the DETA, **1s**, **1a** and **2s** remaining in the liquid phase. *Ex-situ* titration of $CO_2$ and amine in the solid phase, which agrees with values deduced from *in situ* loadings, provide access to the statistical minimal, maximal and average values of the various carbamated states of DETA within the solid (see methods section). These populations can then be combined and compared to the non-templated library to apprehend the template effect exerted by the metal salt on the whole $CO_2$-DETA dynamic system (figure 2b). While the initial trajectory follows the repartition of the reference library, the precipitation phenomenon induces a marked shift, interpreted as the disproportionation of the heterotopic ligand **1a** into the homotopic species DETA and **2s**. This deviation accentuates with increased loading, while **1s** remains almost unaffected. Full molecular analyses of each phase allow to correlate the evolution of the dynamic covalent organic system with the partition of the inorganic species (figure 2c and d). During the disproportionation of **1a** into **2s** and DETA, the metal cation selectively co-precipitates with the former, while chloride remains in solution with the latter (with a selectivity factor defined as the ratio of the partition coefficients $S_{Ln/Cl} = 360$). The formation of the supramolecular

metallo-dicarbamate solid can reasonably designated be as the driving force of this biphasic counter-ion exchange process triggered by $CO_2$ capture. The extent of this complexation-driven disproportionation is provided by the loading dependent amplification factor $AFi(\alpha)$[28] plotted in figure 3a for i = DETA and **2s**. This parameter, which can be defined as

$$AF_i(\alpha) = \frac{x_i(\alpha) - x_i^0(\alpha)}{x_i^{max}(\alpha) - x_i^0(\alpha)}$$

quantifies the metal-induced increase of the molar fraction $x_i$ of a given $CO_2$-amine adduct i with respect to the non-templated library ($x_i^0$). To give some insight on the metal-ligand stoichiometry, this factor was normalized with the molar fraction of metal introduced with respect to the total amount of amine, as an arbitrary maximal increase ($x_i^{max}$-$x_i^0$). Monitoring of this parameter for $CO_2$ loadings where carbonation levels are marginal confirms that rare earth cations selectively bind **2s** with a 2:1 stoichiometry, inducing thereby the disproportionation of 4eq of **1a** and the release of 2 eq. of free DETA with isolated yields reaching 85 % (equation 7, figure 3a and Supplementary material fig.S3).

**Micro- and macroscopic perturbing effects of metal salts: toward a solvent-dependent classification**

Using the same analytical methodology, d-block metals such as nickel and cobalt (both involved with rare earth elements in the composition of key components of batteries) were probed for their ability to micro- and macroscopically perturb the dynamic covalent DETA-$CO_2$ system. At the +2 oxidation degree, these neighbors in the periodic table were previously reported to reversibly bind polyamine-based ligands thereby yielding dynamic combinatorial libraries of octahedral complexes.[29] While rare earth metals collectively display the same behavior,[21] nickel and cobalt afforded soluble systems along the full $CO_2$ loading range in the presence of 12 eq. of DETA. $^1$H and $^{13}$C NMR monitoring reveal that both templates induce the conversion of **1a** into free DETA and to a much lesser extent, into dicarbamate **2s** (Supplementary material fig. S2). This trend, precisely quantified by the amplification factors (figure 3b and c and Supplementary material fig. S3) indicates that metal-induced carbamate hydrolysis proceeds simultaneously during the disproportionation reaction, to a metal-dependent extent. With $NiCl_2$, 6 $H_2O$, the amplification of **2s** is limited to 25 mol% with respect to the template, the dominant reaction being the hydrolysis of carbamates. This cleavage is driven by the formation of the Werner-like complex *mer*-(Ni(DETA)$_2$Cl$_2$, which could be isolated and characterized by X-ray diffraction analyses from the reaction mixture (Supplementary material fig. S4a). In contrast, $CoCl_2$.6$H_2O$ induces the conversion of 3 eq. of monocarbamates into 2 eq. of DETA and 1 eq. of **2s**, which corresponds to a maximal level of carbamate hydrolysis of 33 mol%.

This preliminary analysis suggests that the compositional modification of the DETA-$CO_2$ library is coupled to the aerial oxidation of $Co^{2+}$ into the more oxophilic[30] $Co^{3+}$ species. Such a convergent evolution was confirmed by mass spectrometry, which both confirmed the +3 oxidation state of the metal and its association in the first coordination sphere to non-carbamated DETA ligands. This strongly cationic species equipped with 10 hydrogen-donating sites is a powerful anion binder,[31] whose adducts with chlorides and carbamates were indeed the major species detected in (-)-CSI-MS mode (Supplementary material fig S5). DFT calculation at the B3LYP-D3BJ/def2TZVP level (Supplementary material fig.S10), confirms that the conversion of the Co(dien)$_2$$^{3+}$, **2s**H$^-$, 2Cl$^-$ salt into the heteroleptic complex Co(dien)**2s**Cl and DETA*HCl which implies a ligand exchange in the first coordination sphere is thermodynamically favored. Yet, in their seminal study on double level dynamic libraries based on polyamine-cobalt complexes appended with hydrazones,[16] Eliseev and Lehn precisely exploited the oxidation of cobalt from +2 to +3 states to freeze the metal-ligand exchange. In the present case, free DETA selection and amplification is first directed by $Co^{2+}$ whose first coordination sphere becomes static upon aerial oxidation.[32] The resulting cationic and H-bond donating species, acts as an anion template by selecting and binding **2s** in the second coordination sphere

(as a second dynamic combinatorial process). This subtle yet clearly distinct binding behavior of Ni and Co toward the $CO_2$-DETA system validates the ability of the $CO_2$ capture process to yield on demand tailored combinations of ligand for each metal, and to potentially be valorized for metal separation from mixtures.
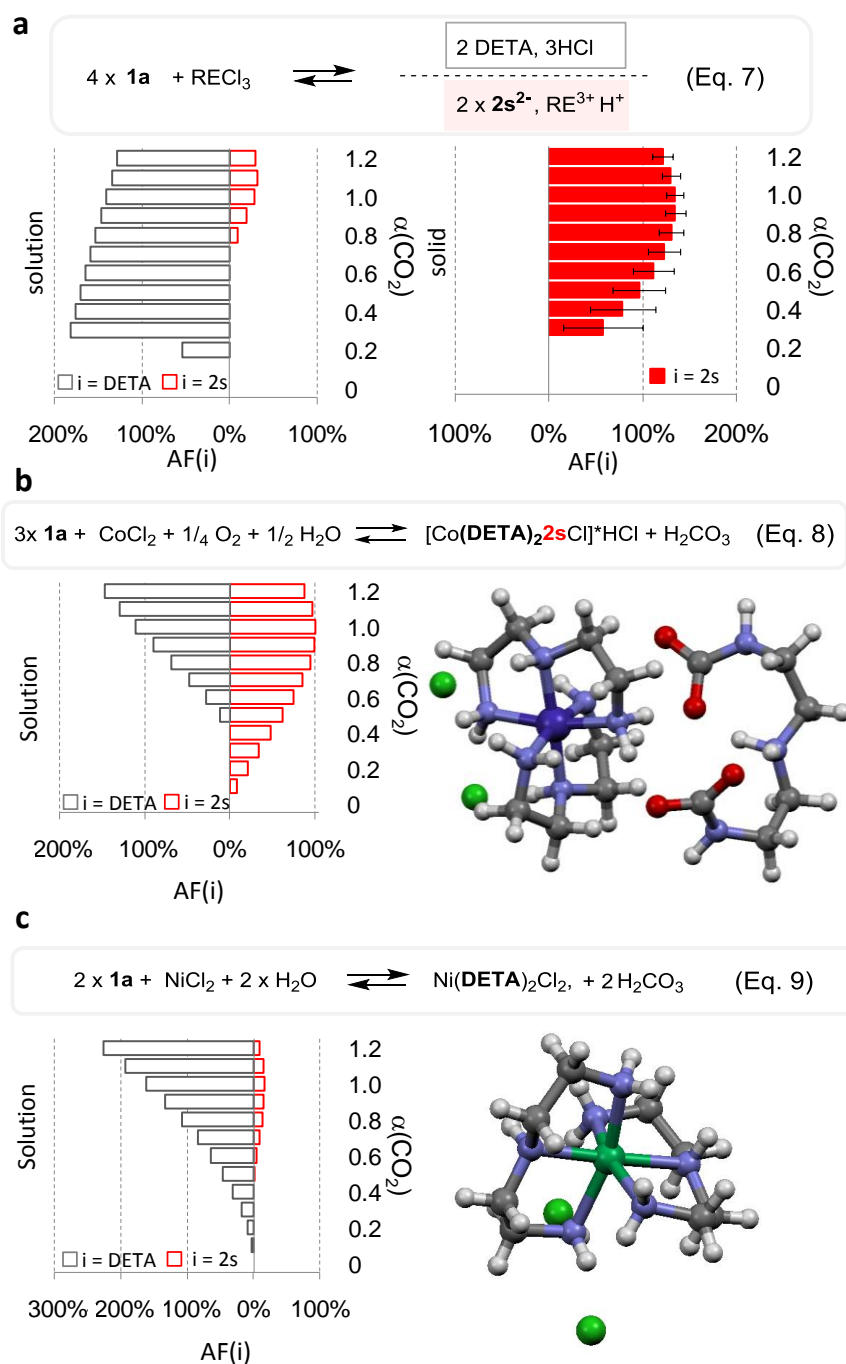


**Figure 3. Perturbations of the $CO_2$-DETA dynamic system by differential complexation processes involving metal chlorides (Eq. 7-9).** Amplification factors of uncarbamated DETA (black) and symmetrical dicarbamate (red) obtained with (a) $RECl_3$ in the supernatant (empty bars) and solid (full bars), in homogeneous solutions with $CoCl_2$ (b) and $NiCl_2$ (c). $Co(DETA)_2\textbf{2s}.HCl$ and *mer*-$Ni(DETA)_2Cl_2$ structures were obtained by DFT calculation at the B3LYP-D3BJ/def2TZVP level and X-ray diffraction spectroscopy.

The classification of each metals salt, according to both its binding preference to a specific combination of members of the $CO_2$-DETA library and its capacity to trigger a phase separation phenomenon, allows to easily rationalize the trends subsequently observed by *ex situ* analyses on bimetallic (La/Ni, La/Co) and trimetallic (La/Ni/Co) systems. In methanol, the

presence equimolar amounts of cobalt inhibits the capture of lanthanum, which occurs at higher $CO_2$ loading (0.75 instead of 0.25) and reduces their maximal capture yield or efficiency is from 95 to 55 %. Yet, cobalt co-capture is limited to 1% of the total amount introduced, which translates into selectivity factors around $10^2$. While both cations should display affinities of the same order of magnitude for **2s**, as indicated by their $AF_{2s}(\alpha>0.25)$ values,[33] $Co^{3+}$ is the only species acting as a **2s**-binder/amplifier at low loading ($\alpha<0.25$), thereby maintaining the amount of unbound **2s** below the solubility limit and consequently postponing the lanthanum-induced capture process by precipitation. Additionally, cobalt presumably acts as a solubilizing agent through the formation of salts between its cationic bis(DETA) adduct and anionic lanthanum polycarbamate anions,[34] thereby decreasing the capture efficiency of the latter at high $CO_2$ loading. In contrast, $NiCl_2$ which binds 8.3% of the total amount of DETA, decreases the $La^{3+}$ capture efficiency by the same order of magnitude through its hydrolytic activity. Nickel and lanthanum represent a typical case of metal-ligand self-sorting, as they select and bind individually each of the carbamate disproportionation products, thereby synergistically amplifying this organic reaction. As a result of the spontaneous phase separation of their respective adducts, nickel and lanthanum cross-contamination in both liquid and solid phases are limited to traces (< 1.2 ppm molar). Selectivities $S_{La/Ni}$ reaching $10^5$ can be obtained, which translates into a purity of the lanthanum recovered by $CO_2$-induced precipitation up to 99.99 %. On the trimetallic equimolar mixture gathering the ingredients found in cathodes of NiMH batteries, the trends from the bimetallic systems are mostly superimposed and are dominated by the Co-La antagonism: lanthanum capture is delayed by the preliminary formation of the cobalt bis(diethylentriamine)-dicarbamate complex, which also limits the maximal yield at high loading, while selectivities with respect to each transition metal are comparable. Saturating the methanolic DETA solutions containing the trimetallic mixture with $CO_2$ consequently leads to the recovery of 56 % of the lanthanum introduced with a 99.50 to 99.90 % purity through a single spontaneous precipitation step.

The polarity of the solvent was then investigated as an experimental lever to sequentially precipitate each metal from solutions through $CO_2$ capture. Moving from methanol to water allows for $CO_2$ hydration to additionally take place, *i.e.* expands the diversity of the $CO_2$-amine systems to ammonium and metal carbonates. In the absence of metal (Supplementary material fig. S6), the dispersive feature of water translates into the decorrelation between **2s** and **1s** and the formation of substantial levels of asymmetrical dicarbamate **2a** and carbonates, the maximal accessible loading thereby exceeding the previous limit $\alpha(CO_2)_{max} = 1.5$. In the presence of $NiCl_2$ and $CoCl_2$, the $CO_2$-DETA system remains macroscopically homogeneous with no apparent perturbation of the population at the molecular level. In contrast, a stepwise process occurs with $YCl_3$: during the first minutes after $CO_2$ introduction, the metal-induced disproportionation of **1a** into DETA and **2s** still proceeds although it is attenuated in comparison to what was observed in methanol. This kinetic regime is characterized by the absence of carbonates up to $\alpha(CO_2) = 1.5$. The transient metal-carbamate homogeneous solutions then progressively relax toward solid-liquid mixtures of thermodynamic products. On the whole loading range, quantitative conversion (> 97 %) into pure insoluble rare earth carbonate tetrahydrate (identified from ex situ pXRD analyses with lanthanum, supplementary material fig. S7a and b) and untemplated metal-free $CO_2$-DETA solution is obtained. Investigations on the La/Co/Ni: 1/1/1 system revealed that selective and quantitative precipitation of rare earth carbonate only occurs with the fully loaded DETA-$CO_2$ system while subsystems formed only from either $CO_2$, NaOH, $Na_2CO_3$ or DETA either lead to unselective co-precipitation of the three metals or to low yield or rare earth capture (Spplementary material fig. S7c). This observation underlines the key role of the library of $CO_2$-DETA based ligands and counter-ions in the self-sorting process, even when inorganic carbonates are to be separated from the medium.
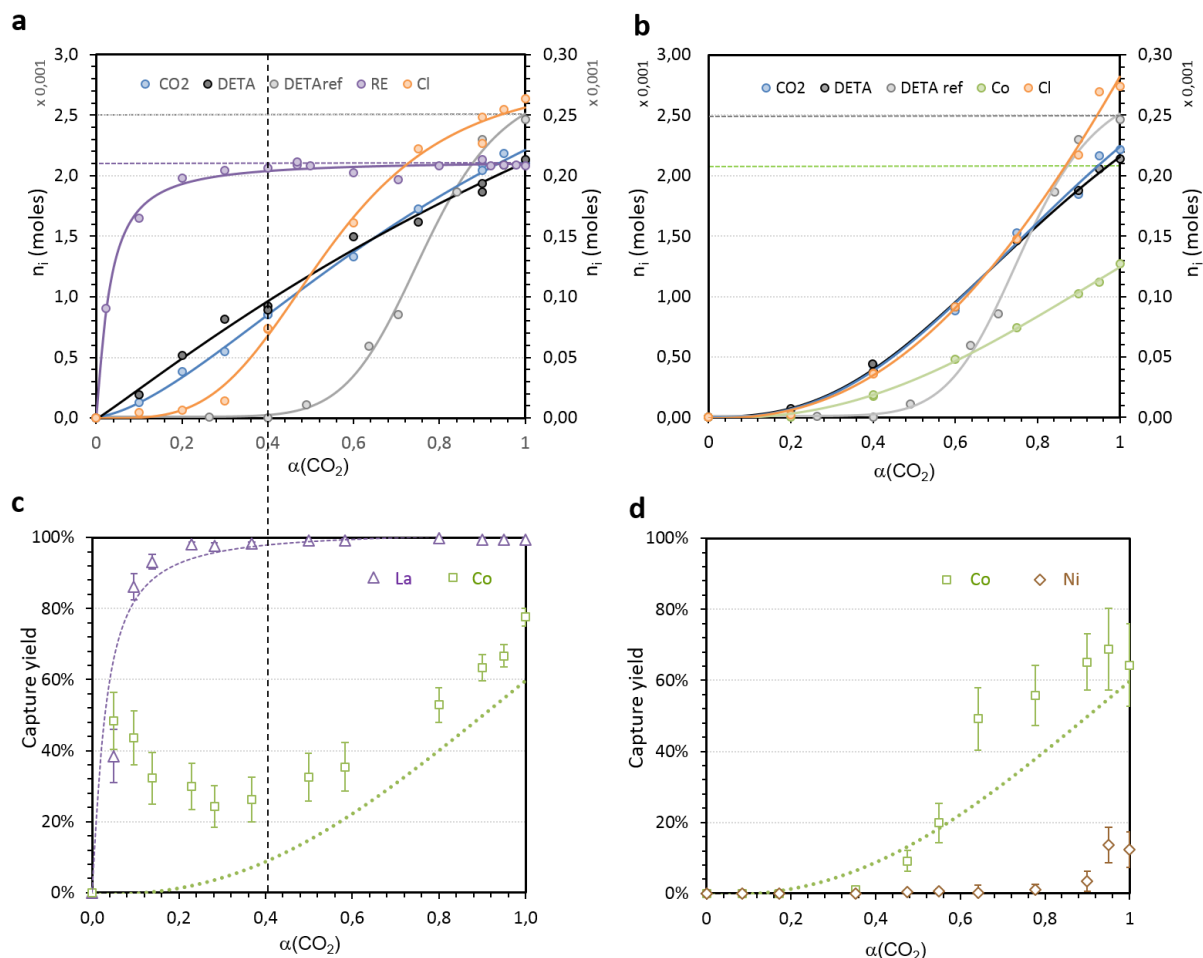
**Figure 4. Building block captures into self-assembled solids from ethanolic solutions of metal chloride(s) (62.5 mM total) with 500 mM DETA on the $\alpha(CO_2)$ = 0-1 loading range**. (a) $LaCl_3, 7H_2O$. (b) $CoCl_2, 6H_2O$. Amounts of DETA captured in the absence of metal (grey) is shown for comparison. Extraction yields of each metal from 62.5 mM 1:1 bimetallic $LaCl_3:CoCl_2$ (c) and $CoCl_2:NiCl_2$ (d) solutions. The vertical dotted line indicates the transition between La-directed and spontaneous carbamate aggregation

The picture changes dramatically when switching to a slightly less dissociative medium such as ethanol. In the absence of metal, a 1:1 mixture of DETA: $CO_2$ precipitates spontaneously on the $\alpha(CO_2)$ = 0.3-1 loading range, yielding a highly hydroscopic amorphous solid which is non-eligible for crystallographic analyses. While such a composition corresponds to the broadest possible statistical distribution between various carbamation states, qNMR monitoring indicates that the speciation and loading of the supernatant remain constant ($\alpha \approx 0.5$) during the process. We hypothesize that, once the solubility limit is reached, each $CO_2$ molecule introduced converts free DETA into a monocarbamate, which co-precipitates with a second molecule of monocarbamate, thereby maintaining the population constant. Such a cooperative aggregation scenario agrees with the sigmoidal yield-to-loading relationship observed. In this system, the addition of $LaCl_3$ induces a marked decrease of the solubility of the organic adducts, which translates into a visible shift (from 0.75 to 0.5) in the half loading of each category of building block, except the metal cation, and to a flattening of the corresponding binding curves (figure 4a). Without perturbing the global $CO_2$: amine stoichiometry of the solid, lanthanum acts as "carbamate glue" by templating a non-cooperative aggregation process. During this preliminary metal-directed regime ($\alpha(CO_2) < 0.3$), which precedes the cooperative self-assembling of the monocarbamate species previously described, 98 % of the lanthanum can be collected into a metal-rich, chloride poor ($S_{La/Cl} > 100$) solid, which then progressively enriches into DETA, $CO_2$ and chloride up to 10, 10 and 1 eq. respectively, with respect to the metal.

In contrast, cobalt behaves as a significantly weaker binder, exerting a much more modest template effect on the carbamate aggregation process. While the $CO_2$: DETA stoichiometry of the solid also remains unaffected, the shifting and flattening of the binding curves followed by each class of building block is significantly attenuated in comparison to the lanthanum-containing system (figure 4b). As regard their partition, cobalt and chloride are unselectively captured on the 0.2-1 loading range, with up to 55 % yield. This "passive incorporation" is also reflected by the $CoCl_2(DETA,CO_2)_{20}$ stoichiometry of the solid, which remains remarkably constant during the full process. Despite its moderate impact comparatively to lanthanum, cobalt confirms its classification as a carbamate binder. In fact, in the exact same conditions, only traces (< 100 ppm) of nickel are incorporated into the self-aggregated monocarbamate phase (Supplementary material fig. S8). Although many grey areas remain to be explored through thorough molecular analyses, we chose to carry on toward the design of a preliminary flowchart of complete polymetallic separation exclusively directed by $CO_2$-capture. We therefore focused on screening for potential optimal loading values, for which each metal may selectively and efficiently be separated from by bi- (La/Co; Co/Ni) and trimetallic (La/Ni/Co) mixtures by precipitation.

Contrary to what happens in methanol, the presence of a competing metal does not decrease the yields for lanthanum, but increases cobalt co-capture from the 1/1: La/Co system (figure 4c). This is particularly dramatic at low $CO_2$ loading ($\alpha < 0.4$) during the lanthanide-directed regime, while the monometallic trend is mostly restored during the organic regime, *i.e.* at higher $CO_2$ loading ($\alpha > 0.4$). The La/Co selectivity values, which reach magnitudes of $10^2$-$10^3$, mostly reflect the excellent efficiency of lanthanum capture (up to 99.8 %), which is yet inevitably hampered by prohibitive levels of contamination with cobalt ($E_{Co}^{min} > 25$ %). On the Co/Ni system (figure 4d), if cobalt capture efficiencies remain modest ($E_{Co}^{max} = 70$ %) and a slight increase in nickel incorporation is observed at high $CO_2$ loading, suitable operational conditions can be found to minimize the latter ($E_{Ni}(0.75) < 0.3$ %) while maintaining fair yields for the former ($E_{Co}(0.75) = 50$ %). The trends observed on these bimetallic mixtures are roughly averaged on the trimetallic La/Ni/Co system: compared to Ni/Co, cobalt capture is increased at low $CO_2$ loading by the template effect exerted by lanthanum, while the levels of nickel incorporation slightly decrease.
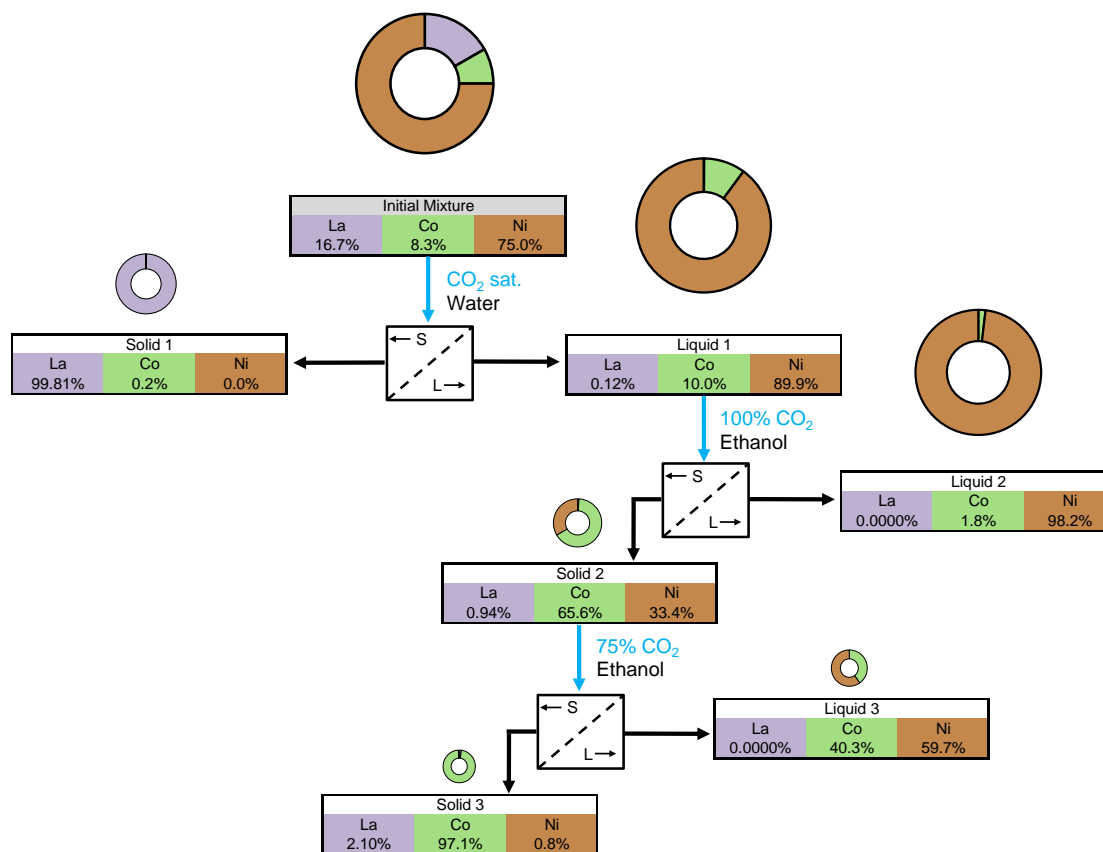
.

**Figure 5. Flowchart of individual metal recovery induced by CO₂ capture from La₂CoNi₉ alloys.** S = solid; L = Liquid. Surface area of the pie charts are proportional to the amount in moles % of the metal contained in the phase concerned with respect to the starting material, while figures in the chart indicate the proportion of each metal in moles %.

This rudimentary screening reveals that although cobalt can selectively be separated from nickel upon $CO_2$ capture, ethanol cannot be envisaged as a unique medium to sequentially precipitate lanthanum, cobalt and nickel with acceptable degrees of purity. To provide the first brick toward a sustainable separation process utilizing $CO_2$-capture as a trigger, recovery of the individual constituents of the La₂CoNi₉ alloy involved in the electrodes of batteries was finally attempted using water and ethanol as successive solvents. Two sequences were investigated: the separation of lanthanum and cobalt from nickel by co-capture in ethanol followed by the selective precipitation of the former in water, and the selective precipitation of lanthanum in water followed by the extraction of cobalt from the Co/Ni leachate upon dilution with ethanol. The second sequence, whose flowchart is represented in Figure 5, was the only one affording acceptable degrees of separation between lanthanum and cobalt. Upon acidic digestion, the trimetallic extracts were diluted with aqueous DETA, which was then saturated with $CO_2$, yielding 99.4 % of the lanthanum initially introduced as a carbonate with a 99.9 % purity (solid 1). Upon stripping and dilution with ethanol, the resulting solution provided two crops: i) the first was triggered by loading DETA with $CO_2$ up to 100 %, and further decrease the polarity of the medium with isopropanol in order to fully precipitate cobalt and thereby maximize the purity of the nickel remaining in solution (liquid 2: Ni(dien)₂Cl₂. 98.3 % purity; 95.3 % yield); and ii) the second resulted from the release of the $Ni^{2+}/Co^{2+}$ mixture entrapped in the monocarbamate solid (solid 2) by thermal stripping of $CO_2$ followed by a capture at the loading previously identified as affording an acceptable efficiency-selectivity tradeoff for cobalt (solid 3; CoCl₂(DETA,CO₂)₂₀. yield : 55.2 % - purity : 97 %). Although a fourth liquid fraction remains as 60/40 Co/Ni residue (liquid 3; 6 % of the total mass processed), this non-optimized sequence underlines the promises held by this new sustainable separating

chemistry. To finally illustrate its flexibility and applicability in the context of integrated $CO_2$ capture and utilization,[35] we briefly investigated the feasibility of direct metal-separation triggered by $CO_2$ capture from flue gas in aqueous DETA. $LaCl_3$:$NiCl_2$ was selected for its ideal self-sorting behavior toward the DETA-$CO_2$ system and the flue gas was directly withdrawn from the exhaust pipe of a an thermic internal combustion engine vehicle set at neutral gear (movie provided in the supporting material). Within minutes, lanthanum carbonate tetrahydrate precipitated and separated from the purple solution of the $Ni(DETA)Cl_2$ complex, both adducts being recovered after phase separation with 99 % yield and 99 % purity (Supplementary material fig. S9. The decrease in yield and purity comparatively the experiments conducted with pure $CO_2$ is imputed to the absence of alkaline scrubbing step devoted to quench sulfur containing gases before $CO_2$ absorption). Concomitant metal purification obviously add a substantial number of additional operations to the global capture process flowsheet, including metal-amine separation.[21] Yet, the value of the co-products which are purified at a 1:1 or even 0.1:1 stoichiometry with respect to $CO_2$ is two to three orders of magnitude higher than the cost of the greenhouse gas, which may leave some appreciable room for potential process integration.

**Integrating $CO_2$-based technologies with capture**

Achieving the objectives set by the international community urgently requires to both cut-off the emissions by accelerating the development of Non-Emitting Technologies and to implement economically viable CCUS pathways in order to capture what has already been emitted or has to be produced. To avoid the pale comparison with fossil-fuel based processes which benefit from centuries of optimization, carbon dioxide has to be considered as a commodity or resource which can afford new objects and systems with unprecedented properties. We herein tried to illustrate that the $CO_2$ absorption step based on amine scrubbing both generates of a library of tailored ligands for metal cations and the associated screening technique. The $CO_2$-stripping step, which is known to be the Achilles's heel of post-combustion capture, also easily allows to free the purified metal from its tailored binding partner in an appreciably more sustainable manner than what conventional hydrometallurgy so far proposed. Although further study will be necessary before a realistic industrial implementation, this integrative approach reveals that innovative $CO_2$-based technologies may be designed with no fossil-sourced equivalent. In the present preliminary study, $CO_2$ may either be recovered as a gas at the end of the multi-step sequence, or stored into metal carbonates produced from waste material. In addition, it is utilized in a way that seems fully compatible with its current most mature technology of post-combustion capture. Integrating its purification with metal separation offers opportunities for appreciable cost saving which may change the game. To finally come back to GHG emission control, metal extraction and recycling is genuine issue in the context of renewable energy transfer and storage, where sustainable and innovative strategies are requested[36] to provide the present and future technological devices with a low impacting life cycle.

**Author contributions** J.L. conceived the idea, J.L and J.S designed the experiments. J.S. and C.T. carried out the experimental work. J.S., C. T. and P. J. conducted the analyses. R.G and C. N. designed and performed the simulations. J.L. and J.S. co-wrote the paper. All authors contributed to revising the paper.

**Competing interests** The authors have filed patent application WO2014188115 relating to this work.

1. COP21. *COP21 Paris France Sustainable Innovation Forum 2015* (2015). Available at: http://www.cop21paris.org
2. International Energy Agency, 2016. 20 years of Carbon Capture and Storage. Accelerating Future Deployment. Paris (France). Available at https://webstore.iea.org/20-years-of-carbon-capture-and-storage.
3. Bottoms, R. R. (Girdler Corp.). Separating acid gases. *U.S. Patent* 1783901, 1930.
4. Rochelle, G. T. Amine scrubbing for $CO_2$ capture. *Science* **325**, 1652-1654 (2009).
5. Jakobsen, J., Roussanaly, S. & Anantharaman, R. A techno-economic case study of $CO_2$ capture, transport and storage chain from a cement plant in Norway. *J. Cleaner Production* **144**, 523-539 (2017).
6. Shulenberger, A.M., Jonsson, F.R., Ingolfsson, O. & Tran, K.-C. Process for producing liquid fuel from carbon dioxide and water. *US Patent Application* 2007/0244208 A1. 2007. http://carbonrecycling.is/george-olah/
7. Lin, Y.-J., Chen, E. & Rochelle, G.T. Pilot plant test of the advanced flash stripper for $CO_2$ capture. *Faraday Discuss.*, **192**, 37-58 (2016)
8. Yang, Z.-Z., He, L.-N., Gao, J., Liua, A.-H. & Yu, B. Carbon dioxide utilization with C–N bond formation: carbon dioxide capture and subsequent conversion. *Energy Environ. Sci.*, **5**, 6602-6639 (2012).
9. McGhee, W., Dennis, R., Christ, K., Pan, Y. & Parnas, B. Carbon Dioxide as a Phosgene Replacement: Synthesis and Mechanistic Studies of Urethanes from Amines, $CO_2$, and Alkyl Chlorides. *J. Org. Chem.* **60**, 2820-2830 (1995).
10. Belli Dell'Amico, D., Calderazzo, F., Labella, L., Marchetti, F. & Pampaloni, G. Converting Carbon Dioxide into Carbamato Derivatives. *Chem. Rev.* **103**, 3857-3898 (2003).
11. Armelao, L., Belli Dell'Amico, D., Biagini, P., Bottaro, G., Chiaberge, S., Falvo, P., Labella, L., Marchetti, F. & Samaritani, S. Preparation of N,N-Dialkylcarbamato Lanthanide Complexes by Extraction of Lanthanide Ions from Aqueous Solution into Hydrocarbons, *Inorg. Chem.* **53**, 4861-4871 (2014).
12. Moreno Pineda, E., Lan, Y., Fuhr, O., Wernsdorfer W. & Ruben M. Exchange-bias quantum tunneling in a $CO_2$-based Dy4-single molecule magnet. *Chem. Sci.* **8**, 1178-1185 (2017).
13. Jessop, P. G., Mercer, S. M. & Heldebrant, D, J. $CO_2$-triggered switchable solvents, surfactants, and other materials, *Energy Environ. Sci.*, **5**, 7240-7253 (2012).
14. Carretti, E., Dei, L., Weiss, G.R. & Baglioni, P. A new class of gels for the conservation of painted surfaces. *J Cult. Herit.*, **9**, 386-393 (2008).
15. H Jung, H. B., Carroll, K. C., Kabilan, S., Heldebrant, D. J., Hoyt, D., Zhong, L., Varga, T., Stephens, S., Adams, L., Bonneville, A., Kuprat, A. & Fernandez, C. A. Stimuli-responsive/rheoreversible hydraulic fracturing fluids as a greener alternative to support geothermal and fossil energy production. *Green. Chem.*, **17**, 2799–2812 (2015).
16. Goral, V., Nelen, M. I., Eliseev, A. V. & Lehn, J.-M. Double-level ''orthogonal'' dynamic combinatorial libraries on transition metal template. *Proc. Nat. Acad. Sci.*, **98,** 1347-1352 (2000).
17. Hartono, A., Hoff, K. A., Mejdell, T., and Svendsen, H. F, Solubility of Carbon Dioxide in Aqueous 2.5 M of Diethylenetriamine (DETA) Solution. *Energy Procedia* **4,** 179‑186, (2011).
18. Leclaire, J., Husson, G., Devaux, N., Delorme, V., Charles, L., Ziarelli, F., Desbois, P., Chaumonnot, A., Jacquin, M., Fotiadu, F. & Buono, G. $CO_2$ Binding by Dynamic Combinatorial Chemistry: An Environmental Selection. *J. Am. Chem. Soc.*, **132**, 3582-3593 (2010).
19. Leclaire, J., Poisson, G., Ziarelli, F., Pepe, G., Fotiadu, F., Paruzzo, F. M., Rossini, A. J., Dumez, J.-N., Elena-Herrmann, B. & Emsley, L. Structure elucidation of a complex $CO_2$-based organic framework material by NMR crystallography. *Chem. Sci.*, **7**, 4379-4390 (2016).
20. J Septavaux, J., Germain, G. & Leclaire, J. Dynamic Covalent Chemistry of Carbon Dioxide: Opportunities to Address Environmental Issues. *Acc. Chem. Res.*, **50**, 1692-1701 (2017).
21. Stern, M. C., Simeon, F., Herzog, H. & Hatton, T. A. Postcombustion carbon dioxide capture using electrochemically mediated amine regeneration. *Energy Environ. Sci.*, **6**, 2505–2517 (2013).
22. Poisson, G., Germain, G., Septavaux, J. & Leclaire, J. Straightforward and selective metal capture through $CO_2$-induced self-assembly. *Green Chem.*, **18**, 6436-6444 (2016).

23. Harper, N. D., Nizio, K. D., Hendsbee, A. D., Masuda, J. D., Robertson, K. N., Murphy, L. J., Johnson, M. B., Pye, C. C. & Clyburne, J. A. C. Survey of Carbon Dioxide Capture in Phosphonium-Based Ionic Liquids and End-Capped Polyethylene Glycol Using DETA (DETA = Diethylenetriamine) as a Model Absorbent. *Ind. Eng. Chem. Res.*, **50**, 2822–2830 (2011).

24. Huc, I. & Lehn, J.-M. Virtual combinatorial libraries: Dynamic generation of molecular and supramolecular diversity by self-assembly. *Proc. Natl. Acad. Sci. U.S.A.*, **94**, 2106–2110 (1997).

25. Vaidya, P. D. & Kenig, E. Y. Termolecular Kinetic Model for $CO_2$-Alkanolamine Reactions: An Overview. *Chem. Engin. Tech.*, **33**, 1577-1581 (2010).

26. Steinhardt, R., Hiew, S. C., Mohapatra, H., Nguyen, D., Oh, Z., Truong R., & Esser-Kahn, A., Cooperative CO2 Absorption Isotherms from a Bifunctional Guanidine and Bifunctional Alcohol. *ACS Cent. Sci.*, **3**, 1271-1275 (2017).

27. Shinoda, S., Terada, K. & Tsukube H., Induced Circular-Dichroism Chirality Probes for Selective Amino Acid Detection through Screening of a Dynamic Combinatorial Library of Lanthanide Complexes. *Chem. Asian J.*, **7**, 400 – 405 (2012).

28. Hamieh, S., Saggiomo, V., Nowak, P., Mattia, E., Ludlow, R. F. and Otto, S., A "Dial-A-Receptor" Dynamic Combinatorial Library. *Angew. Chem. Int. Ed*., **52**: 12368-12372 (2013).

29. Neranon, K. & Ramstrom, O. Kinetics and Thermodynamics of Constitutional Dynamic Coordination Systems Based on $Fe^{II}$, $Co^{II}$, $Ni^{II}$, $Cu^{II}$, and $Zn^{II}$. *Eur. J. Inorg. Chem.*, **24**, 3950‑3956 (2016).

30. Kepp, K. P., A Quantitative Scale of Oxophilicity and Thiophilicity. *Inorg. Chem.*, **55**, 9461–9470 (2016).

31. Keene, F. R. & Searle G. H., Isomers of the Bis(diethylenetriamine)cobalt(III) Cation. Dependence of Equilibrium Isomer Proportions on Environmental Parameters. *Inorg. Chem*.**13**, 2173-2180 (1974).

32. Marusak, R. A., Osvath, P., Kemper, M. & Lappin, A. G. Stereoselectivity in the Reduction of $[Co(ox)_3]^{3-}$ by $[Co(en)_3]^{2+}$ and Its Derivatives. *Inorg. Chem.*, **28**, 1542-1548 (1989).

33. Corbett, P. T., Otto, S. & Sanders, J. K. M., Correlation between Host–Guest Binding and Host Amplification in Simulated Dynamic Combinatorial Libraries. *Chem. Eur. J.*, **10**, 3139-3143 (2004)

34. Wang, Y., Yu, J., Guo, M. & Xu, R. $[\{Zn2(HPO_4)_4\}\{Co(dien)_2\}]\cdot H_3O$: A Zinc Phosphate with Multidirectional Intersecting Helical Channels. *Angew. Chem. Int. Ed*., **42**, 4089-4092 (2003).

35. Mission Innovation CCUS Report, *Accelerating Breakthrough Innovation in Carbon Capture, Utilization, and Storage* (2018) available at https://www.energy.gov/fe/downloads/accelerating-breakthrough-innovation-carbon-capture-utilization-and-storage

36. Sholl, D. S. & Lively, R. P. Seven chemical separations to change the world. *Nature* **532,**435–437 (2016).